



# Tsallis entropy inspires geometric thermodynamics of specific black hole

Shamaila Rani<sup>1,a</sup>, Abdul Jawad<sup>1,b</sup>, Hooman Moradpour<sup>2,c</sup>, Aqsa Tanveer<sup>1,d</sup>

<sup>1</sup> Department of Mathematics, COMSATS University Islamabad, Lahore 54000, Pakistan

<sup>2</sup> Research Institute for Astronomy and Astrophysics of Maragha (RIAAM), University of Maragheh, P.O. Box 55136-553 Maragheh, Iran

Received: 26 February 2022 / Accepted: 10 July 2022

© The Author(s) 2022

**Abstract** In this paper, we analyze the thermodynamics of five-dimensional Schwarzschild AdS black hole in  $AdS_5 \times S^5$  spacetime in the presence of Tsallis entropy. Since the cosmological constant  $\Lambda$  is considered as thermodynamical pressure with volume as its conjugate, but this explanation cannot be employed in AdS/CFT correspondence. In this study, we associate cosmological constant  $\Lambda$  in boundary gauge theory with the number of colors  $N$  and chemical potential is taken to be its thermodynamic conjugate. The two geometric parameters in the AdS black hole,  $r$  and  $L$  are substituted for two thermodynamic parameters in the micro-canonical ensemble, which are considered to be entropy  $S$  and  $N^2$ . Moreover, we evaluate several thermodynamical geometry formulations, including Weinhold, Ruppeiner, and Quevedo and derive associated scalar curvatures for five-dimensional Schwarzschild AdS black hole. It is suggested that all these geometries show repulsive/attractive forces on the particles at different phases of entropy.

## 1 Introduction

The Hawking's area theorem suggested that the area of a black hole (BH) is analogous to entropy. These findings confirmed the area theorem is an outcome of the second law of thermodynamics by representing that the entropy is related to the area of the event horizon. It actually paved the way for BH thermodynamics and the proportionality constant was set after the discovery of Hawking radiation. The ultimate formulation of Bekenstein entropy and Hawking temperature is as follows [1–4]

$$T_H = \frac{\hbar c^3}{8\pi G k_B M}, \quad S = \frac{c^3 k_B A_H}{4G\hbar}. \quad (1)$$

Here,  $\hbar$  shows Planck's constant, the Newton's constant is denoted by  $G$ ,  $c$  represents the speed of light,  $k_B$  shows the Boltzmann constant,  $A_H$  is area of event horizon and  $M$  is the mass of BH.

Thermodynamics of BHs has been an intriguing discipline of study for researchers lately, explicitly after when scientists have been treated the cosmological constant as pressure  $P = -\frac{\Lambda}{8\pi}$ . This is when the first law of BH thermodynamics was procured. The thermodynamics of BHs began with the pioneering work of Bekenstein and Hawking on the relationship between entropy  $S$  and area  $A$  and temperature  $T$  and surface gravity  $\kappa$  of the event horizon [4–6]. While generalizing Komar's concept of mass of asymptotically flat AdS space-times, an important feature of BH thermodynamics emerges, namely the necessity of a dynamical cosmological constant. Black holes in anti-de Sitter (AdS) space have very different thermodynamical characteristics than BHs in asymptotically flat or de Sitter space. The major explanation is because AdS space behaves as a confined cavity, allowing BHs to remain thermodynamically stable in AdS space. In the correspondence of AdS/CFT, a negative cosmological constant  $\Lambda$  is associated with  $N$ , the degrees of freedom of the dual conformal field theory (CFT).

In the case of  $AdS_5 \times S^5$  and the finite temperature  $\mathcal{N} = 4$  of the superconformal Yang–Mills theory at large  $N$ , it seems more appropriate to view a dynamical  $\Lambda$  as the varying number of colors of the dual CFT and its conjugate associated to chemical potential  $\mu$ , conjugate to the number of colors in the frame of reference of Schwarzschild BH  $AdS_5 \times S^5$ , the chemical potential in the Yang–Mills theory's high temperature phase is discovered to be negative and diminishes as temperature rises [10,11]. Also, when the temperature falls below the Hawking–Page temperature, it was observed that the chemi-

<sup>a</sup> e-mail: shamailatoor.math@yahoo.com (corresponding author)

<sup>b</sup> e-mails: jawadab181@yahoo.com; abduljawad@cuilahore.edu.pk

<sup>c</sup> e-mail: hn.moradpour@maragheh.ac.ir

<sup>d</sup> e-mail: tanveeraqsa708@gmail.com

cal potential of spherical BHs in the bulk approaches to zero and the heat capacity divergence changes the sign at a temperature around that point.

Applying geometrical principles to conventional thermodynamical systems, on contrary, provides a new means of studying phase transition in such systems. Many scholars have contributed to the development of this methodology. Since BHs are thought to be thermodynamic systems, it makes sense to examine their thermodynamic geometries. Previous research suggests that the thermodynamic geometry of BHs has a structure from which scientific conclusions may be deduced [12]. In equilibrium states, Hermann [13] established a differential manifold as an interconnection of thermodynamic phase space with a natural contact structure of subspace. Weinhold [14] was the first to develop a metric based on the second derivatives of internal energy regarding entropy and other thermodynamic parameters. Ruppeiner [15] presented another metric, the negative Hessian of entropy and other extensive variables of a thermodynamic system, based on the fluctuation theory of thermodynamic equilibrium process.

In contrast to more traditional techniques, Ruppeiner geometry is a macroscopic probe that may be used to figure out the nature of interactions in a thermodynamic system [16]. Furthermore, the Weinhold metric was demonstrated to be conformal to the Ruppeiner metric [17]. However, under Legendre transformation, both the Weinhold and Ruppeiner metrics are not invariant, and occasionally contradicting findings are obtained [18]. Numerous efforts were made, with the ultimate result being a non-invariant metric under Legendre transformations [19]. Quevedo proposed that by using purely mathematical principles, both techniques may be combined into a single approach. This method is known as geometrothermodynamics, and it is a unifying technique that allows us to interpret thermodynamics in a geometric terminology, whether at the phase space level or in the space of equilibrium states. The phase transition of BHs was studied by using the thermodynamical geometry technique [20–23]. We have also investigated different phenomenon of the BHs in various theories of gravity [24–31].

This manuscript is structured in such a way that we explore the thermodynamics and thermodynamical geometry of a five-dimensional Schwarzschild AdS BH with respect to Tsallis entropy in  $AdS_5 \times S^5$  considering the number of colors as a thermodynamical variable from the perspective of dual CFT. In Sect. 2, we briefly describe Tsallis entropy and covers the thermodynamical properties of a BH in  $AdS_5 \times S^5$  taking the cosmological constant  $\Lambda$  as number of colors  $N$ . In Sect. 3, we compute the scalar curvatures of various metrics for the thermodynamical system to evaluate their relationships with phase transition. In support of our study, physical interpretations are also provided. In Sect. 4, concluding arguments of the study are discussed.

## 2 Tsallis entropy and thermodynamic properties

The entropy of a BH has fascinating elements that have been debated for decades and assertions have been made that the BH entropy is related to the area of its boundary rather than the BH volume. Hawking demonstrated the emission of black body radiations with a temperature by relating quantum matter fields to a classical BH. The Bekenstein–Hawking entropy can be expressed as

$$S_{BH} = \frac{k_B}{4} \frac{A_H}{G\hbar/c^3}. \quad (2)$$

Here,  $A_H$  represents the area of event horizon and  $G$  is Newton's constant,  $k_B$  appears as Boltzmann constant,  $\hbar$  shows the reduced Planck constant,  $c$  is the speed of light. Indeed, since the fundamental ideas of Bekenstein and Hawking, there has been a widespread recognition in the literature that the BH entropy is unconventional in the sense that it breaches thermodynamical extensivity. Thus, if the system is physically defined as (d-1)-dimensional, then the additive entropy  $S_{BG}$  must be considered as its thermodynamical entropy. However, if the system is to be physically regarded as d-dimensional,  $S_{BG}$  cannot be recognized as its thermodynamical entropy, and a nonadditive entropy is required to serve that role. From a historical point of view, the thermodynamical deviation associated with the area law is generally overlooked. However, there are several scientific and mathematical facts that identify such a viewpoint as anomalous. To obtain an approach to overcome the issue, for such complex systems, it is sufficient to associate the thermodynamical entropy with nonadditive entropies like  $S_q$  rather than the standard Boltzmann–Gibbs–von Neumann (additive) entropy is not proportional to the volume for highly entangled systems, black holes, and systems obeying the area law in general. The thermodynamical entropy cannot be identified with the conventional one in such strongly correlated systems but with a significantly different (nonadditive) one. In order to maintain thermodynamic extensivity for nonstandard systems, entropies generalizing those of BG become essential. Tsallis and Cirto [32] demonstrated that a BH's horizon entropy may be manipulated as

$$\frac{S_q}{k_B} \propto \left( \frac{S_{BG}}{k_B} \right)^{d/d-1} \quad (d > 1), \quad (3)$$

where  $S_q$  and  $S_{BG}$  denote Tsallis and Boltzmann–Gibbs entropy respectively. Tsallis suggested that it can be linked to the renowned Bekenstein–Hawking entropy  $S_{BH}$  such as

$$\frac{S_q}{k_B} \propto \left( \frac{S_{BH}}{k_B} \right)^\delta. \quad (4)$$

Equation (4) may be expressed as follows

$$S_q = \Gamma A^\delta, \quad (5)$$

where,  $\delta$  indicates the non-additivity parameter and  $\Gamma$  is an arbitrary constant. Bekenstein entropy is clearly retrieved at the specified limit of  $\delta = 1$  and  $\Gamma = 1/4G$  (in the system when  $\hbar = k_B = c = 1$ ).

The Schwarzschild metric, discovered by Karl Schwarzschild in 1916, is an ultimate solution to the Einstein field equations that explains the gravitational field beyond a spherical mass under the assumption that all quantities, the universal cosmological constant, electric charge and angular momentum are zero. A static Schwarzschild BH has neither angular momentum nor electric charge. Substantial advancement in higher-dimensional space-time physics has been accomplished, following the proposal of the five-dimensional Schwarzschild BH metric. The Schwarzschild-AdS solution is the most basic example of an asymptotically AdS BH which is presented as follows [33–35]

$$ds^2 = -g(r)dt^2 + g(r)^{-1}dr^2 + r^2d\Omega^2_3. \quad (6)$$

Metric function  $g(r)$  is given by [36]

$$g(r) = k - \frac{8G_5M}{3\pi r^2} + \frac{r^2}{L^2}, \quad (7)$$

where  $L$  is length scale in  $AdS_5$  space-time, with cosmological constant  $\Lambda = -\frac{6}{L^2}$ ,  $k$  is scalar curvature parameter and it can take values as  $-1, 0$  or  $1$ . Here  $M$  is the mass of BH, and  $G_5$  indicates the five-dimensional Newton's constant. Now, one must know that, in accordance with AdS/CFT five-dimensional Newton's constant  $G_5$  is also a function of  $L$

$$\frac{1}{16\pi G_5} = \frac{V_{S^5}}{16\pi G_{10}},$$

where,  $V_{S^5} = \pi^3 L^5$ , volume of five-dimensional sphere with radius  $L$ , which gives  $G_5 = \frac{G_{10}}{\pi^3 L^5}$  where  $G_{10}$  is the fixed ten-dimensional Newton's constant linked to ten-dimensional Planck's length  $l_p$  as:  $G_{10} = l_p^{-8}$ . The relation between AdS radius  $L$  and D-3-branes can be specified by [37]

$$L^4 = \frac{\sqrt{2}Nl_p^4}{\pi^2}, \quad (8)$$

In above relation,  $l_p$  denotes ten-dimensional Planck length which is constant throughout. The following equation, Eq. (9) can be derived using, Eqs. (3) to (5)

$$S = \Gamma \left( \frac{\pi^5 r^3 L^5}{2l_p^8} \right)^\delta. \quad (9)$$

In compliance with AdS/CFT correspondence, the space-time Eq. (7) is considered as the gravity dual to  $\mathcal{N} = 4$  Superconformal Yang–Mills theory, at finite temperature with large  $N$ .  $N$  denotes the rank of the gauge group of the  $SU(N)$  super-symmetric Yang–Mills theory. In above relations, although cosmological constant  $\Lambda$  is normally taken to be fixed, however, in  $AdS_5 \times S^5$ , it is not a priority but just

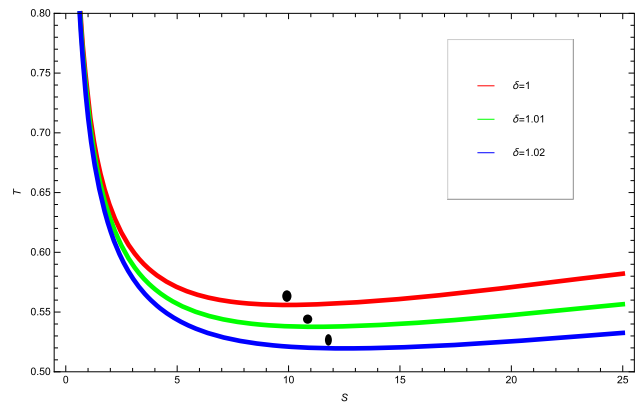


**Fig. 1** The temperature with respect to entropy with  $k = 1$ ,  $l_p = 1$ ,  $\Gamma = 1$  and  $N = 3$

a parameter as any constant in 10-dim super-gravity solutions and can be varied. In, thermodynamic energy of the boundary CFT was computed as the function of the volume  $V$ , temperature  $T$  and  $N$ . While the bulk metric has only one parameter, keeping  $\Lambda$  fixed and even  $\Lambda$  is allowed to vary, we are left with two parameters which are not enough. It entails a presumption. The ideology here is to use entropy  $S$  and  $N^2$  as an alternative for the parameter congenital to the BHs such as  $r$  and  $L$ . The mass of BH can be obtained by taking  $g(r) = 0$  in Eq. (7)

$$M = \frac{3\pi^4 r^2 L^3 (kL^2 + r^2)}{8G_{10}}. \quad (10)$$

## 2.1 Mass and temperature

Substituting values from Eqs. (9) and (8) in Eq. (10), we get the mass of BH in terms of  $N$  and  $S$  as follows

$$M(S, N) = \frac{3\tilde{m}_p}{4\Gamma^{\frac{4}{3\delta}}\delta\pi} \left\{ kN^{\frac{5}{12}} \left( \frac{S}{\pi} \right)^{\frac{2}{3}} \Gamma^{\frac{2}{3\delta}} S^{\frac{2(1-\delta)}{3\delta}} + \left( \frac{S}{\pi} \right)^{\frac{4}{3}} N^{-\frac{11}{12}} S^{\frac{4(1-\delta)}{3\delta}} \right\}. \quad (11)$$

Here  $\tilde{m}_p = \frac{\sqrt{\pi}m_p}{2^{\frac{1}{8}}}$  with  $m_p = \frac{l_p^7}{G_{10}}$  represents the Planck mass with 10-dimensions. The Hawking temperature follows

$$T = \frac{\partial M}{\partial S} \Big|_N,$$

$$T = \frac{\tilde{m}_p}{2\Gamma^{\frac{4}{3\delta}}\delta\pi} \left\{ kN^{\frac{5}{12}} \Gamma^{\frac{2}{3\delta}} \left( \frac{S}{\pi} \right)^{-\frac{1}{3}} S^{\frac{2(1-\delta)}{3\delta}} + 2N^{-\frac{11}{12}} \left( \frac{S}{\pi} \right)^{\frac{1}{3}} S^{\frac{4(1-\delta)}{3\delta}} \right\}. \quad (12)$$

The Fig. 1 shows the relationship between Hawking temperature and entropy. It can be seen from the graph that tem-

perature gets a minimum value which indicates that it does not show monotonic behavior.

- For  $\delta = 1$ , we get minimal temperature  $T = 0.52$  at  $S = 10$ .
- For  $\delta = 1.01$ , we obtain minimal temperature  $T = 0.54$  at  $S = 11$ .
- For  $\delta = 1.02$ , minimum value of temperature is  $T = 0.56$  at  $S = 12$ .

Notably, we do not find any BH solution below this minimal temperature. There are two branches above the minimal temperature, the branch having small entropy is unstable whereas the large entropy shows thermodynamical stability.

## 2.2 Gibbs free energy

The Gibbs free energy is a thermodynamic quantity that may be used to measure the maximum reversible work that a thermodynamic system can accomplish at a certain temperature and pressure. The Gibbs free energy is considered to be a promising state function to use when comparing configurations in the grand canonical ensemble. The Gibbs free energy is a significant thermodynamic quantity to evaluate BH global stability. Now, the Gibbs-free energy  $G$  is found by the relation [38]

$$G = M - TS,$$

Here  $M$ ,  $T$  and  $S$  are mass, temperature and entropy of the BH respectively. Its expression for this BH becomes

$$G(T, N^2) = \left[ \frac{3\tilde{m}_p}{4\Gamma^{\frac{4}{3\delta}}} \left\{ kN^{\frac{5}{12}} \left( \frac{S}{\pi} \right)^{\frac{2}{3}} \Gamma^{\frac{2}{3\delta}} S^{\frac{2(1-\delta)}{3\delta}} \right. \right. \\ \left. \left. + \left( \frac{S}{\pi} \right)^{\frac{4}{3}} N^{-\frac{11}{12}} S^{\frac{4(1-\delta)}{3\delta}} \right\} \right] \\ - \left[ \frac{\tilde{m}_p}{2\Gamma^{\frac{4}{3\delta}} \delta} \left\{ kN^{\frac{5}{12}} \Gamma^{\frac{2}{3\delta}} \left( \frac{S}{\pi} \right)^{\frac{2}{3}} S^{\frac{2(1-\delta)}{3\delta}} \right. \right. \\ \left. \left. + 2N^{-\frac{11}{12}} \left( \frac{S}{\pi} \right)^{\frac{4}{3}} S^{\frac{4(1-\delta)}{3\delta}} \right\} \right].$$

Figure 2 depicts the relation between Hawking temperature and Gibbs free energy. We can see that Gibbs free energy changes its sign at a point analogous to Hawking–Page transition point. Figure shows the following observations.

- For  $N^2 = 4$ ,  $G$  increases at  $T = 0.66$  that is its phase transition point and decreases in the interval  $[0.63, 1.15]$ . However, Gibbs free energy exhibits the global stability of BH in the interval  $[0.63, 1.15]$  with respect to temperature.
- For  $N^2 = 9$ ,  $G$  increases at  $T = 0.6$  analogous to transition point and decreases in the interval  $[0.55, 1.325]$ . In

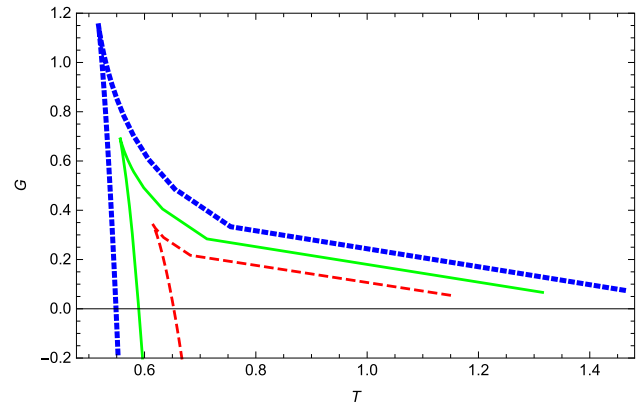


**Fig. 2** The Gibbs free energy with respect to temperature for discrete number of colors with  $k = 1, l_p = 1, \Gamma = 1$  taking  $N^2 = 4$  (red dashed line);  $N^2 = 9$  (green solid line);  $N^2 = 16$  (blue dotted line)

this case, global stability of BH appears in the interval  $[0.55, 1.325]$  for temperature.

- For  $N^2 = 16$ ,  $G$  increases at  $T = 0.55$ , at this point it undergoes phase transition and decreases in the interval  $[0.53, 1.5]$  (where global stability appears).

## 2.3 Chemical potential

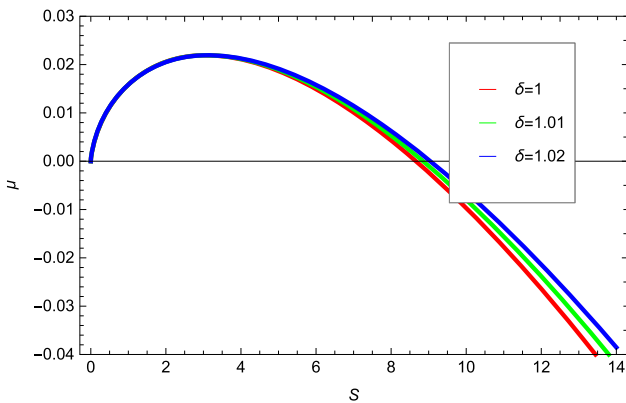
The chemical potential  $\mu$  can be calculated by taking derivative of  $M$  with respect to  $N^2$ . Thus,

$$\mu = \frac{\partial M}{\partial N^2} \Big|_S, \\ \mu = \frac{\tilde{m}_p}{32\Gamma^{\frac{4}{3\delta}}} \left\{ 5kN^{-\frac{19}{12}} \left( \frac{S}{\pi} \right)^{\frac{2}{3}} \Gamma^{\frac{2}{3\delta}} S^{\frac{2(1-\delta)}{3\delta}} \right. \\ \left. - 11 \left( \frac{S}{\pi} \right)^{\frac{4}{3}} N^{-\frac{35}{12}} S^{\frac{4(1-\delta)}{3\delta}} \right\}. \quad (13)$$

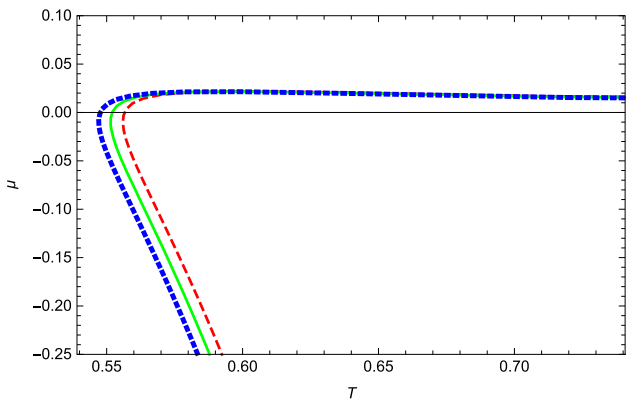
$N^2$  has been taken instead of  $N$ , since in the boundary  $\mathcal{N} = 4$  supersymmetric Yang–Mills Theory, all the fields are represented as  $SU(N)$ .  $\mu$  is nothing but energy cost to the system by the increment of the number of colors.

Figure 3 illustrates the behavior of chemical potential with respect to entropy, while  $N$  is fixed. One can see that for  $\delta = 1$ , chemical potential gets positive values with respect to small values of  $S$  and it changes sign at 8.75 and becomes negative. Starting from  $S = 0$ , the chemical potential experiences positive behavior in the interval  $0 \leq S \leq 8.75$  which is the stable branch and changes to negative from this point onwards in the unstable branch.

We plot Fig. 4 to examine the relation of chemical potential  $\mu$  with temperature  $T$ . We study the behavior of chemical potential as a function of temperature in the range  $[0.54–0.75]$  and get to the following conclusions.



**Fig. 3** The chemical potential with respect to entropy by taking  $N = 3$  while  $k = 1$ ,  $\Gamma = 1$  and  $l_p = 1$



**Fig. 4** The chemical potential  $\mu$  with respect to temperature  $T$  while  $k = 1$ ,  $\Gamma = 1$  and  $l_p = 1$ , with  $N = 3$  (red dashed line);  $N = 3.1$  (green solid line);  $N = 3.2$  (blue dotted line)

- For  $N = 3$ ,  $\mu < 0$  in  $(0.555, 0.592]$ ,  $\mu = 0$  at  $T = 0.555$  and  $\mu > 0$  in  $(0.555, 0.75]$
- For  $N = 3.1$ ,  $\mu < 0$  in  $(0.553, 0.588]$ ,  $\mu = 0$  at  $T = 0.553$  and  $\mu > 0$  in  $(0.553, 0.75]$
- For  $N = 3.2$ ,  $\mu < 0$  in  $(0.548, 0.582]$ ,  $\mu = 0$  at  $T = 0.548$  and  $\mu > 0$  in  $(0.548, 0.75]$

It can be verified that at the Hawking–Page temperature, chemical potential approaches to zero. In addition, the Hawking–Page transition happens in the large BH branch, while the chemical potential is zero in the small BH branch.

Figure 5 is plotted to analyze the behavior of chemical potential  $\mu$  with respect to  $N$  with a fixed entropy  $S$ . The chemical potential has its maximum value at  $N \approx 2.9$  and declines when  $N$  increases. It can be seen that chemical potential  $\mu$  is negative for  $1 \leq N \leq 2$  and becomes positive in the interval  $(2, 20]$ .

#### 2.4 Heat capacities

The specific heat is a popular merit to investigate the thermal stability. The heat capacity ought to be positive which

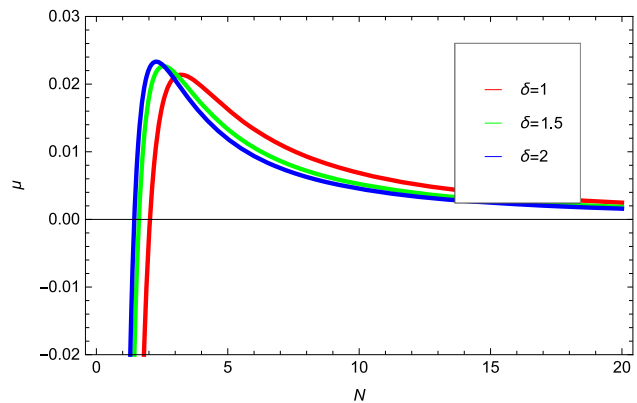


**Fig. 5** The chemical potential with respect to  $N$  for entropy value as  $S = 4$

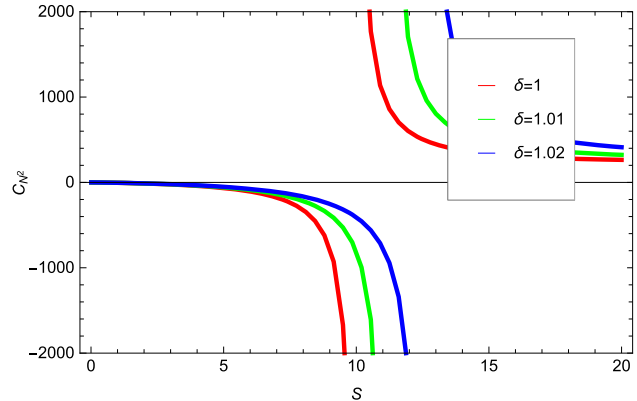


**Fig. 6** The heat capacity with respect to entropy by taking  $N = 3$

represents a thermally stable system [39]. The heat capacity of the black hole paves the way to the analysis of the phase transition. The specific heat of the system at constant  $N^2$  can be specified as

$$C_{N^2} = T \left( \frac{\partial S}{\partial T} \right)_{N^2},$$

$$C_{N^2} = - \frac{3S\delta(2S^{\frac{2}{3\delta}} + kN^{\frac{4}{3}}\pi^{\frac{2}{3}}\Gamma^{\frac{2}{3\delta}})}{kN^{\frac{4}{3}}\pi^{\frac{2}{3}}\Gamma^{\frac{2}{3\delta}}(-2 + 3\delta) + S^{\frac{2}{3\delta}}(-8 + 6\delta)}. \quad (14)$$

Taking  $\delta = 1$ ,  $\Gamma = 1$  and  $k = 1$ , the Eq. (14) reduces to the expression Eq. (3.1) of [36].

Figure 6 represents heat capacity versus entropy with  $N$  as a fixed value. Heat capacity is negative in a region where  $S$  is small and it diverges to become positive when  $S$  increases.

- For  $\delta = 1$ ,  $C_{N^2} < 0$  in  $[4, 9.5]$ ,  $C_{N^2} = 0$  in  $[0, 4]$  and  $C_{N^2} > 0$  in  $[11, 20]$ .
- For  $\delta = 1.01$ ,  $C_{N^2} < 0$  in  $[4, 10.6]$ ,  $C_{N^2} = 0$  in  $[0, 4]$  and  $C_{N^2} > 0$  in  $[12, 20]$ .
- For  $\delta = 1.02$ ,  $C_{N^2} < 0$  in  $[4, 11.9]$ ,  $C_{N^2} = 0$  in  $[0, 4]$  and  $C_{N^2} > 0$  in  $[13.6, 20]$ .

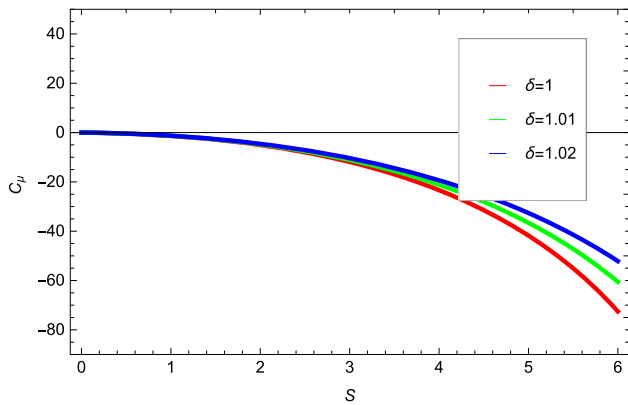


**Fig. 7** The heat capacity with respect to entropy  $S$  by taking  $N = 3$ ,  $k = 1$ ,  $\Gamma = 1$  and  $l_p = 1$

The negative heat capacity indicates instability of BH system while its positive sign ensures that BH system is stable. We can see a close similarity between the divergence point of heat capacity and minimum Hawking temperature.

Also, specific heat of the system keeping chemical potential  $\mu$  fixed can be obtained as

$$C_\mu = \left( \frac{\partial \phi}{\partial T} \right)_\mu,$$

where  $\phi = M - \mu N^2$ .

$$C_\mu = - \frac{S\delta(70S^{\frac{2}{3\delta}} + 19kN^{\frac{4}{3}}\pi^{\frac{2}{3}}S^{\frac{2}{3}}\Gamma^{\frac{2}{3\delta}})}{8(kN^{\frac{4}{3}}\pi^{\frac{5}{3}}\Gamma^{\frac{2}{3\delta}}(-2 + 3\delta) + S^{\frac{2}{3\delta}}\pi(-8 + 6\delta))}. \quad (15)$$

The heat capacity as a function of entropy is plotted in Fig. 7, keeping  $\mu$  fixed. It can be seen that  $C_\mu$  decreases as  $S$  increases, also  $C_\mu = 0$  for  $0 \leq S \leq 1$  and changes to negative onwards. It is suggested that BH shows stability in the range  $0 \leq S \leq 1$  and exhibits instability for  $S > 1$ .

### 3 Thermodynamic Geometry of the Schwarzschild AdS BH

Let us move towards the BHs thermodynamical geometry to check whether the thermodynamical curvature may disclose the singularity of heat capacities. The geometric evaluation of equilibrium phase spaces plays a key role in aspects of modern thermodynamic research.

#### 3.1 Weinhold geometry

Weinhold space-time is taken as internal energy with its second derivative in relation to entropy and other substantial quantities. Weinhold geometry is illustrated as follows [14]

$$g_{ij}^W = \partial_i \partial_j M(S, N^2). \quad (16)$$

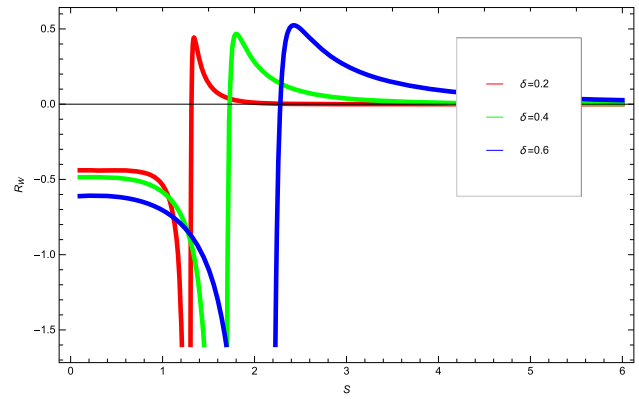


**Fig. 8** The scalar curvature with respect to entropy  $S$  for Weinhold space-time by taking  $k = 1$ ,  $N = 3$ ,  $\Gamma = 1$  and  $l_p = 1$

The line element for the Schwarzschild AdS BH can be revised as

$$ds^2_W = M_{SS}dS^2 + M_{N^2N^2}d(N^2)^2 + 2M_{SN^2}dSdN^2. \quad (17)$$

which, in matrix form can be represented as

$$\begin{pmatrix} M_{SS} & M_{SN^2} \\ M_{NS^2} & M_{N^2N^2} \end{pmatrix}. \quad (18)$$

Using above equations, one can find out curvature scalar of Weinhold metric as

$$R = \frac{A}{B}, \quad (19)$$

where  $A$  and  $B$  are as follows

$$\begin{aligned} A = & 160/3(N^{\frac{9}{4}}\pi^2k(-554S^{\frac{2(3\delta+4)}{3\delta}}\Gamma^{\frac{8}{3\delta}}N^{\frac{4}{3}}\pi^{\frac{2}{3}}k \\ & + 2068S^{\frac{2(3\delta+5)}{3\delta}}\Gamma^{\frac{2}{3}} \\ & + 1195S^{\frac{2(3\delta+4)}{3\delta}}\Gamma^{\frac{8}{3\delta}}N^{\frac{4}{3}}\pi^{\frac{2}{3}}k\delta - 4466S^{\frac{2(3\delta+5)}{3\delta}}\Gamma^{\frac{2}{3}}\delta \\ & + 641S^{\frac{2(3\delta+4)}{3\delta}}\Gamma^{\frac{8}{3\delta}}N^{\frac{4}{3}}\pi^{\frac{2}{3}}k\delta^2 \\ & + 2398S^{\frac{2(3\delta+5)}{3\delta}}\Gamma^{\frac{2}{3}}\delta^2, \\ B = & S^2m(95S^{\frac{4}{3\delta}}N^{\frac{8}{3}}\pi^{\frac{4}{3}}\Gamma^{\frac{4}{3\delta}}k^2\delta - 80S^{\frac{4}{3\delta}}N^{\frac{8}{3}}\pi^{\frac{4}{3}}\Gamma^{\frac{4}{3\delta}}k^2 \\ & - 195S^{\frac{2}{3}}N^{\frac{4}{3}}\pi^{\frac{2}{3}}\Gamma^{\frac{2}{3\delta}}k\delta \\ & + 150S^{\frac{2}{3}}N^{\frac{4}{3}}\pi^{\frac{2}{3}}\Gamma^{\frac{2}{3\delta}}k - 770S^{\frac{8}{3\delta}}\delta + 704S^{\frac{8}{3\delta}})^2. \end{aligned}$$

We can deduce following results from Fig. 8 about Weinhold metric's scalar curvature as:

- For  $\delta = 0.2$ , the curvature scalar has transition point at  $S = 1.3$  and becomes positive.
- For  $\delta = 0.4$ , the curvature scalar has reached a transition point at  $S = 1.7$  and becomes positive.
- For  $\delta = 0.6$ , the curvature scalar has transition point at  $S = 2.2$  and turns positive.

Positive scalar curvature indicates the repulsion behavior while negative curvature scalar suggests attraction behavior. Both behaviors are observed for the present BH through Weinhold geometry.

### 3.2 Ruppeiner geometry

We need to analyze the Ruppeiner geometry for the above mentioned BH which is set up as a major thermodynamic potential [15]. Ruppeiner proposed that the concept of a metric on the spaces of thermodynamic equilibrium states arises when the idea of fluctuations is incorporated in the axioms of equilibrium thermodynamics. The Ruppeiner metric favors spaces of thermodynamic equilibrium states giving rise to the idea of a length between the states, that is the probability of fluctuation between couple of thermodynamic states varies inversely to the distance between them. It turns out that the curvature scalar  $R$  associated with Ruppeiner geometry incorporates information regarding phase transitions and critical points [40–43]. Furthermore, the divergence of  $R$  has been claimed to suggest a strong relation to the microscopic degrees of freedom. While strength of interactions can be measured by computing absolute value of  $R$ . Lately, this geometry has been applied to different BHs systems [44–49]. A temperature conformal factor connects the Ruppeiner metric to the Weinhold geometry as [50]

$$ds^2_R = \frac{1}{T} ds^2_W. \quad (20)$$

The Ruppeiner metric can be expressed in matrix form as

$$g^R = \frac{1}{T} \begin{pmatrix} M_{SS} & M_{SN^2} \\ M_{NS^2} & M_{N^2N^2} \end{pmatrix}, \quad (21)$$

and the corresponding curvature scalar of the above metric can be calculated as

$$R = \frac{A_1}{B_1}, \quad (22)$$

where  $A_1$  and  $B_1$  are as follows

$$\begin{aligned} A_1 &= kN^{\frac{4}{3}}\pi^{\frac{2}{3}}S^{-1+\frac{2}{3\delta}}\Gamma^{\frac{2}{3\delta}}(-60kN^{\frac{4}{3}}\pi^{\frac{2}{3}}S^{\frac{4}{3\delta}}\Gamma^{\frac{2}{3\delta}} \\ &\quad \times (70 - 603\delta + 582\delta^2) \\ &\quad - 44S^{\frac{2}{\delta}}(896 + 5\delta(-354 + 1798)) \\ &\quad + 5k^3N^4\pi^2\Gamma^{\frac{2}{\delta}}(-448 + \delta(330 + 233\delta)) \\ &\quad - 15k^2N^{\frac{8}{3}}\pi^{\frac{4}{3}}S^{\frac{2}{3\delta}}\Gamma^{\frac{4}{3\delta}}(-140 + \delta(-128 + 359\delta))), \\ B_1 &= (2S^{\frac{2}{3\delta}} \\ &\quad + kN^{\frac{4}{3}}\pi^{\frac{2}{3}}\Gamma^{\frac{2}{3\delta}})\delta(15kN^{\frac{4}{3}}\pi^{\frac{2}{3}}S^{\frac{2}{3\delta}}\Gamma^{\frac{2}{3\delta}}(-10 + 13\delta) \\ &\quad - 5k^2N^{\frac{8}{3}}\pi^{\frac{4}{3}}\Gamma^{\frac{4}{3\delta}}(-16 + 198) \\ &\quad + 22S^{\frac{4}{3\delta}}(-32 + 35\delta))^2. \end{aligned}$$

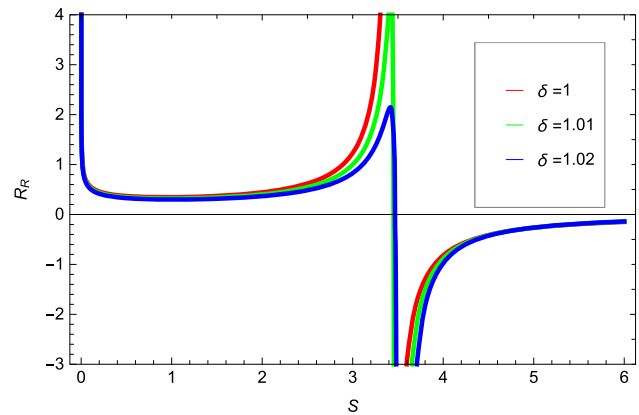


**Fig. 9** The scalar curvature with respect to entropy for Ruppeiner metric by taking  $N = 3$ ,  $\Gamma = 1$ ,  $l_p = 1$  and  $k = 1$

The scalar curvature of Ruppeiner metric is plotted in Fig. 9. As shown in figure, it is clearly visible that scalar curvature diverges at  $S \approx 3.5$ . The curvature scalar of the Ruppeiner metric is positive from  $0 \leq S \leq 3.5$ , where it has a singularity point, and it turns negative from this point forward, as seen in the graph. It means that the trajectories exhibit the attraction behavior of particles by a BH in the range of entropy  $0 \leq S \leq 3.5$ , while repulsive force exerted on the particles by BH for  $S > 3.5$ .

### 3.3 Quevedo geometry

Quevedo [51–53] presented a technique to derive a thermodynamical metric using a Legendre invariant thermodynamic potential. Let  $(2n + 1)$ -dimensional thermodynamic phase space  $\mathcal{T}$  whose coordinates can be presented by the set  $Z^A = \{\phi, E^a, I^a\}$ , where  $A = 0, \dots, 2n$  and  $a = 1, \dots, n$ . In the set of coordinates,  $\phi$ ,  $E^a$  and  $I^a$  identify thermodynamic potential, set of extensive and intensive variables, respectively. In addition, Gibbs 1-form on the space  $\mathcal{T}$  can be presented as  $\Theta = d\phi - \delta_{ab}I^a dE^b$  having  $\delta_{ab} = \text{diag}(1, 1, \dots, 1)$ . The  $(\mathcal{T}, \Theta)$  is known as contact manifold [13, 54] undergoing the conditions that  $\mathcal{T}$  meets the differentiability condition while  $\Theta$  meets the constraint of being non-zero of  $\Theta \wedge (d\Theta)^n$  factor. The set  $\{\mathcal{T}, G, \Theta\}$  can describe a phase manifold or the Riemannian contact manifold [55]. Because of Legendre invariance, the geometric features of metric  $G$  has no effect on the choice of thermodynamic potential in its construction when  $G$  serves on the space  $\mathcal{T}$  as a non-degenerate Riemannian metric. Resulting an  $n$ -dimensional submanifold  $\mathcal{E}$  induced by the mapping  $\varphi : \mathcal{E} \rightarrow \mathcal{T}$ , i.e.,  $\varphi : (E^a) \mapsto (\phi, E^a, I^a)$  satisfying the condition  $\varphi^*(\Theta) = 0$ . One can obtain the non-degenerate Riemannian metric as  $G = (d\phi - \delta_{ab}I^a dE^b)^2 + (\delta_{ab}E^a I^b)(\eta_{cd} dE^c dI^d)$  with  $\eta_{cd} = \text{diag}(-1, 1, \dots, 1)$ .

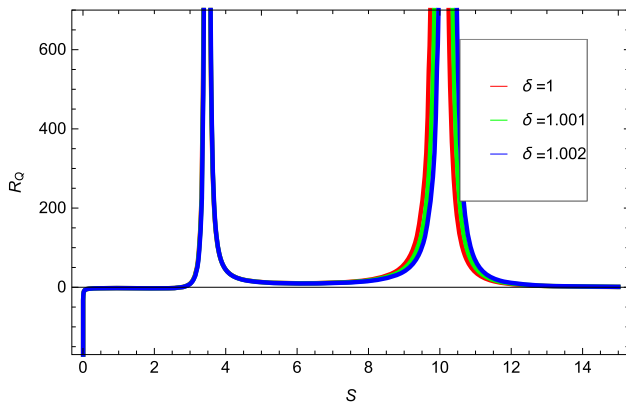


**Fig. 10** The scalar curvature with respect to entropy for the framework of Quevedo metric by taking  $N = 3$ ,  $\Gamma = 1$ ,  $l_p = 1$  and  $k = 1$

Then Quevedo metric can be computed as follows

$$g = \varphi^*(G) = \left( E^c \frac{\partial \phi}{\partial E^c} \right) \left( \eta_{ab} \delta^{bc} \frac{\partial^2 \phi}{\partial E^c \partial E^d} dE^a dE^d \right), \quad (23)$$

The above equation can also be written as

$$g^Q = (ST + N^2 \mu) \begin{pmatrix} -M_{SS} & 0 \\ 0 & M_{N^2 N^2} \end{pmatrix}, \quad (24)$$

The scalar curvature of Quevedo metric may be calculated as

$$R = \frac{A_2}{B_2}, \quad (25)$$

where  $A_2$  and  $B_2$  are given as

$$\begin{aligned} A_2 = & 768(2^{\frac{1}{4}})(3^{\frac{5}{6}})\pi^{\frac{7}{3}}S^{\frac{-2}{38}}\Gamma^{\frac{10}{38}} \left( 108\pi^{\frac{4}{3}}S^{\frac{2}{38}}\Gamma^{\frac{4}{38}} \right. \\ & \times (-744 - 34878 + 4824\delta^2) \\ & + 22(3^{\frac{1}{3}})S^{\frac{2}{3}}(2406 - 75298 + 5304\delta^2) \\ & - 81(3^{\frac{1}{3}})\pi^2\Gamma^{\frac{2}{3}}(-5310 - 10378 \\ & + 8088\delta^2 + (3\pi)^{\frac{2}{3}}S^{\frac{4}{38}}\Gamma^{\frac{2}{38}} \\ & \times (-3550 - 2377418 + 321624\delta^2) \left. \right), \\ B_2 = & 35(77S^{\frac{2}{38}} - 57(3^{\frac{1}{3}})\pi^{\frac{2}{3}}\Gamma^{\frac{2}{38}})^2 (S^{\frac{2}{38}} \\ & + 3(3^{\frac{1}{3}})\pi^{\frac{2}{3}}\Gamma^{\frac{2}{38}})^3 (3(3^{\frac{1}{3}})\pi^{\frac{2}{3}}\Gamma^{\frac{2}{38}}(-2 \\ & + 3\delta) + S^{\frac{2}{38}}(-8 + 6\delta)^2). \end{aligned}$$

The scalar curvature of Quevedo metric diverges at two different points  $S \approx 3.5$  and  $S \approx 10$ . The divergence point  $S \approx 10$  coincides with the zero of  $C_{N^2}$ . The following results are shown in Fig. 10.

- $R_Q < 0$  at  $S = 0$ .
- $R_Q = 0$  in  $(0, 2] \cup [12, 14]$ .
- $R_Q > 0$  in  $(2, 12)$ .

All the results obtained by graphical evaluation are consistent with our study.

#### 4 Conclusions

This work has been devoted to discuss the thermodynamics and thermodynamic geometries of five-dimensional Schwarzschild-AdS black hole in  $AdS_5 \times S^5$  spacetime in correspondence with AdS/CFT in which we have treated cosmological constant  $\Lambda$  as  $N$  (which represents supersymmetric Yang-Mills theory's number of colors at finite temperature for  $\mathcal{N} = 4$ ). We have computed basic thermodynamic parameters in terms of  $S$  and  $N^2$  replacing the geometric parameters  $r$  and  $L$ .

- We have found the relationship between Hawking temperature and entropy. It is observed that temperature has a minimal value which implies that temperature is not a monotonic function.
- We have evaluated Gibbs free energy  $G$  associated with Hawking temperature  $T$  to find out that it changes its sign in correlation with Hawking-Page transition point. Also, Gibbs free energy has shown stable behavior of BH globally.
- We have examined the behavior of chemical potential  $\mu$  which remains negative with respect to BH thermodynamics's stable branch. Although this potential may be positive in the unstable branch.
- Chemical potential with respect to entropy shows positive behavior versus small values of  $S$  and it changes sign at  $S = 8.75$  and becomes negative.
- The behavior of chemical potential with respect to temperature was investigated. Chemical potential gets zero value at the Hawking-Page temperature.
- With a constant entropy  $S$ , we have observed the behavior of chemical potential with respect to  $N$ . The chemical potential is maximum at 2.9 and decreases as  $N$  increases.
- We have also worked out the heat capacities with fixed number of colors  $N$  and with fixed chemical potential  $\mu$ . The former diverges when BH experience minimum value of temperature while the later was seen to be decreasing with the increase in  $S$ .
- We have analyzed the thermodynamic geometries of Weinhold, Ruppeiner and Quevedo metric. It is suggested that all these geometries show repulsive/attractive forces on the particles at different phases of entropy. We have concluded from the interpretation of curvature scalars of all these metrics that identified divergence points for Weinhold, Ruppeiner and Quevedo metric scalar curvatures are comparable to heat capacity divergence points.

**Data Availability Statement** This manuscript has no associated data or the data will not be deposited. [Authors' comment: All the related data has been mentioned in the manuscript.]

**Open Access** This article is licensed under a Creative Commons Attribution 4.0 International License, which permits use, sharing, adaptation, distribution and reproduction in any medium or format, as long as you give appropriate credit to the original author(s) and the source, provide a link to the Creative Commons licence, and indicate if changes were made. The images or other third party material in this article are included in the article's Creative Commons licence, unless indicated otherwise in a credit line to the material. If material is not included in the article's Creative Commons licence and your intended use is not permitted by statutory regulation or exceeds the permitted use, you will need to obtain permission directly from the copyright holder. To view a copy of this licence, visit <http://creativecommons.org/licenses/by/4.0/>.

Funded by SCOAP<sup>3</sup>. SCOAP<sup>3</sup> supports the goals of the International Year of Basic Sciences for Sustainable Development.

## References

1. K. Schwarzschild, On the gravitational field of a mass point according to Einstein's theory. (1999). arXiv preprint [arXiv:physics/9905030](https://arxiv.org/abs/physics/9905030)
2. R.P. Kerr, Gravitational field of a spinning mass as an example of algebraically special metrics. *Phys. Rev. Lett.* **11**(5), 237 (1963)
3. J.M. Bardeen, B. Carter, S.W. Hawking, The four laws of black hole mechanics. *Commun. Math. Phys.* **31**(2), 161–170 (1973)
4. J.D. Bekenstein, Black holes and the second law. *Lettere al Nuovo Cimento* **4**, 737–740 (1972)
5. J.D. Bekenstein, *Phys. Rev. D* **7**, 2333–2346 (1973)
6. S.W. Hawking, *Commun. Math. Phys.* **43**, 199–220 (1975)
7. B.P. Dolan, Bose condensation and branes. *J. High Energy Phys.* **10**, 179 (2014)
8. C.V. Johnson, Holographic heat engines. *Class. Quantum Gravity* **31**(20), 205002 (2014)
9. D. Kastor, S. Ray, J. Traschen, Chemical potential in the first law for holographic entanglement entropy. *J. High Energy Phys.* **2014**(11), 1–17 (2014)
10. A. Belhaj, M. Chabab, H. El Moumni, K. Masmar, M.B. Sedra, On thermodynamics of AdS black holes in M-theory. *Eur. Phys. J. C* **76**(2), 1–9 (2016)
11. S.W. Wei, B. Liang, Y.X. Liu, Critical phenomena and chemical potential of a charged AdS black hole. *Phys. Rev. D* **96**(12), 124018 (2017)
12. S.W. Hawking, Gravitational radiation from colliding black holes. *Phys. Rev. Lett.* **26**(21), 1344 (1971)
13. R. Hermann, *Geometry, Physics, and Systems*, vol. 18 (M. Dekker, New York, 1973)
14. F. Weinhold, Metric geometry of equilibrium thermodynamics. *J. Chem. Phys.* **63**(6), 2479–2483 (1975)
15. G. Ruppeiner, Thermodynamics: a Riemannian geometric model. *Phys. Rev. A* **20**(4), 1608 (1979)
16. G. Ruppeiner, Riemannian geometry in thermodynamic fluctuation theory. *Rev. Mod. Phys.* **67**(3), 605 (1995)
17. P. Salamon, J. Nulton, E. Ihrig, On the relation between entropy and energy versions of thermodynamic length. *J. Chem. Phys.* **80**(1), 436–437 (1984)
18. P. Salamon, E. Ihrig, R.S. Berry, A group of coordinate transformations which preserve the metric of Weinhold. *J. Math. Phys.* **24**(10), 2515–2520 (1983)
19. R. Mrugala, J.D. Nulton, J.C. Schön, P. Salamon, Statistical approach to the geometric structure of thermodynamics. *Phys. Rev. A* **41**(6), 3156 (1990)
20. R.G. Cai, J.H. Cho, Thermodynamic curvature of the BTZ black hole. *Phys. Rev. D* **60**(6), 067502 (1999)
21. N. Pidokrajt, J.E. Aman, I. Bengtsson, Geometry of black hole thermodynamics. *Gen. Relativ. Gravit.* **35**(10), 1733–1743 (2003)
22. J.E. Aman, N. Pidokrajt, Geometry of higher-dimensional black hole thermodynamics. *Phys. Rev. D* **73**(2), 024017 (2006)
23. G. Ruppeiner, Thermodynamic curvature and black holes, in *Breaking of Supersymmetry and Ultraviolet Divergences in Extended Supergravity* (Springer, Cham, 2014), pp. 179–203
24. A. Jawad, M. Tasleem, S. Rani, Consequences of barrow entropy on thermodynamics of charged AdS black hole and heat engine. *Mod. Phys. Lett. A* **37**, 2250062 (2022)
25. A. Jawad, S.R. Fatima, Thermodynamic geometries analysis of black holes with barrow entropy. *Nucl. Phys. B* **976**, 115697 (2022)
26. A. Jawad, G. Abbas, I. Siddique, G. Mustafa, Critical points of regular black hole with Gauss–Bonnet effected entropy. *Eur. Phys. J. Plus* **137**, 284 (2022)
27. S. Chaudhary, A. Jawad, M. Yasir, Thermodynamic geometry and Joule–Thomson expansion of black holes in modified theories of gravity. *Phys. Rev. D* **105**, 024032 (2022)
28. A. Jawad, K. Jusufi, M.U. Shahzad, Accretion of matter onto black holes in massive gravity with Lorentz symmetry breaking. *Phys. Rev. D* **104**, 084045 (2021)
29. A. Jawad, S. Chaudhary, K. Bamba, Impact of Thermal fluctuations on logarithmic corrected massive gravity charged black hole. *Entropy* **23**, 1269 (2021)
30. M. Yasir, K. Bamba, A. Jawad, Thermodynamic properties of modified Hairy and BTZ black holes. *Int. J. Mod. Phys. D* **30**, 2150068 (2021)
31. A. Jawad, Consequences of thermal fluctuations of well-known black holes in modified gravity. *Class. Quantum Gravity* **37**, 185020 (2020)
32. C. Tsallis, L.J. Cirto, Black hole thermodynamical entropy. *Eur. Phys. J. C* **73**(7), 1–7 (2013)
33. R. Emparan, H.S. Reall, Black holes in higher dimensions. *Living Rev. Relativ.* **11**(1), 1–87 (2008)
34. B.P. Dolan, Bose condensation and branes. *J. High Energy Phys.* **11**(1), 1–87 (2014)
35. S. Mahish, A. Ghosh, C. Bhamidipati, Thermodynamic curvature of the Schwarzschild-AdS black hole and Bose condensation. *Phys. Lett. B* **811**, 135958 (2020)
36. J.L. Zhang, R.G. Cai, H. Yu, Phase transition and thermodynamical geometry for Schwarzschild AdS black hole in AdS 5 S 5 spacetime. *J. High Energy Phys.* **2015**(2), 1–16 (2015)
37. J. Maldacena, The large-N limit of superconformal field theories and supergravity. *Int. J. Theor. Phys.* **38**(4), 1113–1133 (1999)
38. M. Zhang, Thermodynamical stability of f(R)-AdS black holes in grand canonical ensemble. *Gen. Relativ. Gravit.* **51**(1), 1–13 (2019)
39. Y.S. Myung, Thermodynamics of the Schwarzschild-de Sitter black hole: thermal stability of the Nariai black hole. *Phys. Rev. D* **77**(10), 104007 (2008)
40. H. Janyszek, R. Mrugaa, Riemannian geometry and stability of ideal quantum gases. *J. Phys. A Math. Gen.* **23**(4), 467 (1990)
41. G. Ruppeiner, Application of Riemannian geometry to the thermodynamics of a simple fluctuating magnetic system. *Phys. Rev. A* **24**(1), 488 (1981)
42. H. Janyszek, R. Mrugal, Riemannian geometry and the thermodynamics of model magnetic systems. *Phys. Rev. A* **39**(12), 6515 (1989)
43. H. Janyszek, Riemannian geometry and stability of thermodynamical equilibrium systems. *J. Phys. A Math. Gen.* **23**(4), 477 (1990)

44. A. Ghosh, C. Bhamidipati, Thermodynamic geometry and interacting microstructures of BTZ black holes. *Phys. Rev. D* **101**(10), 106007 (2020)
45. A. Bravetti, F. Nettel, Thermodynamic curvature and ensemble nonequivalence. *Phys. Rev. D* **90**(4), 044064 (2014)
46. X.Y. Guo, H.F. Li, L.C. Zhang, R. Zhao, Microstructure and continuous phase transition of a Reissner–Nordstrom-AdS black hole. *Phys. Rev. D* **100**(6), 064036 (2019)
47. S.W. Wei, Y.X. Liu, R.B. Mann, Repulsive interactions and universal properties of charged anti-de Sitter black hole microstructures. *Phys. Rev. Lett.* **123**(7), 071103 (2019)
48. S.H. Hendi, S. Panahiyan, B.E. Panah, M. Momennia, A new approach toward geometrical concept of black hole thermodynamics. *Eur. Phys. J. C* **75**(10), 1–12 (2015)
49. B. Mirza, M. Zamaninasab, Ruppeiner geometry of RN black holes: flat or curved? *J. High Energy Phys.* **2007**(06), 059 (2007)
50. B. Mirza, H. Mohammadzadeh, Ruppeiner geometry of anyon gas. *Phys. Rev. E* **78**(2), 021127 (2008)
51. H. Quevedo, Geometrothermodynamics. *J. Math. Phys.* **48**(1), 013506 (2007)
52. H. Quevedo, Geometrothermodynamics of black holes. *Gen. Relativ. Gravit.* **40**(5), 971–984 (2008)
53. H. Quevedo, A. Sánchez, S. Taj, A. Vázquez, Phase transitions in geometrothermodynamics. *Gen. Relativ. Gravit.* **43**(4), 1153–1165 (2011)
54. W.L. Burke, W.L. Burke, W.L. Burke, *Applied Differential Geometry* (Cambridge University Press, Cambridge, 1985)
55. G. Hernández, E.A. Lacomba, Contact Riemannian geometry and thermodynamics. *Differ. Geom. Appl.* **8**(3), 205–216 (1998)